Probable Fungal Colonization and Carbonate Diagenesis of Neoproterozoic Stromatolites from South Gabon, Western Congo Basin

5

Kamal Kolo, Kurt Konhauser, Jean-Pierre Prian, and Alain Préat

5.1 Introduction

Fungi are able to colonize any number of rock surfaces in their efforts to extract nutrients and trace metals for their metabolism. Their filaments, called hyphae, physically exploit grain boundaries, cleavages and cracks to gain access to new mineral surfaces, and in the process, they cause several alteration features, ranging from simple surface roughing by etching and pitting to selective mineral dissolution and cavity formation to extensive physical disintegration of the minerals (see Konhauser 2007 for details). Simultaneously, all exposed mineral surfaces become covered in EPS, which serves to retain water and fuel hydrolysis reactions (Welch et al. 1999). Through the release of organic acids, such as oxalic acid or citric acid (Richter et al. 2007), mineral dissolution is accelerated because the acids dissociate and release protons that can attack minerals directly by complexing with ligands at the minerals surface. Deprotonated organic anions (e.g., oxalate, citrate) indirectly affect dissolution rates by complexing with metal cations in solution, thereby lowering the mineral's saturation state (e.g., Bennett et al. 1988). These interactions not only result in the slow alteration of the primary mineral surfaces, but frequently they induce the formation of secondary mineral phases, such as Ca- and Mg-oxalate and calcite (Gadd 1999; Verrecchia 2000; Chen et al. 2000; Burford et al. 2003a; Hoffland et al. 2004) or the so-called desert varnish comprising Fe- and Mn-oxides (Krumbein and Jens 1981; Grote and Krumbein 1992). Finally, extreme bioweathering can even form a new diagenetic "mycogenic rock fabric" (Burford et al. 2003b).

As weathering agents, fungi have played a particularly important role in the alteration of carbonate rocks: the biodeterioration of carbonate monuments and buildings (Hoffland et al. 2004; Sterfinger and Krumbein 1997), bioerosion of corals and sediment particles (Vogel et al. 2000; Golubic et al. 2005), and the accumulation of carbonate-sourced metals (Sterflinger 2000; Gadd 2007), are just a few examples. The large quantities of oxalic acid produced by fungi can also react with carbonate host rocks to yield Ca-oxalates crystals or re-precipitation of Ca-minerals in the form of calcretes (Verrecchia 2000). Indeed, it has been suggested that fungi are probably at the origin of much the calcium carbonate accumulation in paleosols and $CaCO_3$ enrichment of surficial sediments throughout the Phanerozoic (Verrecchia et al. 2003; Cardon and Whitbeck 2007). For instance, paleosols in the Lower Carboniferous of South Wales contain needle-fibre calcite as coatings on sediment grains and rhizocretions (Wright 1986,). The fibres were probably formed by the calcification of fungal hyphae. Esteban and Klappa (1983) illustrated fungal hyphae in a Pleistocene caliche hardpan from Spain. A well-developed biogenic structure (sparmicritization), related to the activity of fungi and algae is reported by Kahle (1977) on the Pleistocene Miami Limestone which has been transformed into calcareous crusts. Part of the spar-micritization was caused by boring of sparry calcite cement by fungi, followed by in situ calcification. Fossilized fungal hyphae and spores have also been observed in the Upper Devonian of the Rocky Mountains (Canada), in the Lower Carboniferous of northern France and in the Cretaceous of Central Italy by Préat

K. Kolo (✉)
Faculty of Science and Engineering, Department of Petroleum Geosciences, Soran University, Erbil-Soran, Iraq
e-mail: kamal.kolo@soran.edu.iq

K. Konhauser
Department of Earth and Atmospheric Sciences, University of Alberta, Edmonton, AB, Canada
e-mail: kurtk@ualberta.ca

J.-P. Prian
Bureau Recherches Géologiques et Minières, 3 Av Claude Guillemin, BP 36009, 45060 Orléans, Cedex2, France
e-mail: jp.prian@brgm.fr

A. Préat
Département des Sciences de la Terre et de l'Environnement, Université Libre de Bruxelles, CP160/02, Av. F.-D. Roosevelt, 50, 1050 Bruxelles, Belgium
e-mail: apreat@ulb.ac.be

M.J. de Wit et al. (eds.), *Geology and Resource Potential of the Congo Basin*, Regional Geology Reviews,
DOI 10.1007/978-3-642-29482-2_5,

et al. (2003). The fungi are systematically associated with calcrete levels at the top of thin shallowing-upward evaporitic tidal sequences, and their roles in biomineralization were dominant as indicated by particular coated grains, bridging grains, rhizoconcretions, sparmicritization, micritization, perforations and secondary calcite formation from excreted fungal Ca-oxalates.

Despite their importance, it is surprising that only a few detailed studies have been undertaken with the view of assessing carbonate alteration features induced by fungal growth. For instance, Burford et al. (2003a) investigated the role of fungi in the transformation of Paleozoic limestones and dolostones, showing that fungal dissolution of the carbonate substrates led to the formation of new microfabrics, such as polymorphic growth patterns with mineralized hyphae and crystalline material (Na plate-like and Ca-blocky crystals) adhering to their external walls. Although the precise mechanisms involved in the formation of these new 'mycogenic' fabrics were not described, it seems that both metabolism-dependent and metabolism-independent processes played integral roles. Kolo et al. (2007) described the formation of small pits and alveolar structure related to the dissolution of dolomite crystals by fungi of Carboniferous aged dolostones, and showed that the pits were occupied by a dense network of fungal hyphae penetrating the dolomitic substrate and circumventing the grain boundaries through dissolution paths.

There has similarly been a paucity of study directed to observing fossilized fungal communities in the ancient rock record, in part due to a bias directed at the more common and easily recognizable land plants (Taylor et al. 2005) and the difficulties at resolving whether fungal forms in ancient sediments can be reasonably considered "fungi" from one or more of the four classical phyla: Ascomycota, Basidiomycota, Chytridiomycota, and Zygomycota which comprise the so-called true "Fungi" (Cavalier-Smith 1987). At present, the oldest definitive fungal fossils are associated with lichen-like symbiosis is reported from the Doushantuo Formation dated at 600 Ma (Yuan et al. 2006). Butterfield (2005) re-interpreted the presence of *Tappania* in the Mesoproterozoic Roper Group of Australia and extended the record of putative fungi to 1430 Ma. Along with other Proterozoic acritarchs exhibiting fungal-like characteristics (e.g. *Trachyhystrichosphaera, Shuiyousphaeridium, Dictyosphaera, Foliomorpha*), this author considered that there is a case to be made for an extended and relatively diverse record of Proterozoic fungi. However, these reports were later discounted (Cavalier-Smith 2006), leaving us with a reasonably confident fungal phylogeny (Glomalean fungi: Redecker et al. 2000) dating back to ca. 600 Ma. Berbee and Taylor (2001) also suggested such a Neoproterozoic age for this colonization. Compared to this, nearly two decades ago, the oldest reliable fossil fungal finding was from the Devonian Rhynie chert (Stubblefield and Taylor 1988). Other recent studies describe zygomycetes fungal forms from macerations of Late Riphean (Neoproterozoic) raising thus again the issue of when Fungi first appear on Earth (Hermann and Podkovyrov 2006). Given this lack of a reliable Fungi fossil record, and identification problems, the answer is perhaps better resolved through molecular genetics., Based on protein fungal sequence analysis, Heckman et al. (2001) extended all major fungal group lineages back to ca. 1 Ga, and inferred a fungal colonization of Earth deep into the Precambrian. Nevertheless, compelling fossil evidence to corroborate this hypothesis has not been produced to date (Krings et al. 2013).

Finally, little attention has been given to fossilized fungal communities or to their role in carbonate diagenesis (Krumbein 1972); and studies of fungal activity in carbonate sediments older than the Quaternary are relatively limited in number. Our study of the Neoproterozoic of South Gabon revealed numerous per-mineralized fungal relicts: sporangia, sporangiophores, columellae, zygosporangia, suspensors, dichotomous hyphae and spores in the upper part of shallowing-upward evaporitic peritidal sequences. It provides a detailed evaluation of the fungal role in an attempt to better understand the mechanisms involved in the paleo-weathering of a Neoproterozoic carbonate substrate. As documented below, comparison of our observations with in vitro experiments allow us to define an eogenetic sequence driven by fungal invasion and colonization of a Neoproterozoic substrate. This finding, corroborated by comparison with present day fungal-mineral surface interactions, also bears upon the role of microbial activity in the shaping of the late Neoproterozoic Earth surface.

5.2 Geological Setting

The Nyanga synclinorium is an important geotectonic unit of southern Gabon, consisting of a 250 km long deformed basinal structure. It formed during the West Congolian orogeny, which forms a vast Neoproterozoic (Pan-African) metamorphic belt stretching from Angola, in the south, some 2,000 km northwards to Gabon (Thiéblemont et al. 2009; Préat et al. 2011a; and de Wit and Linol, Chap. 2, this Book). The Gabonese part of the belt, averaging 100 km in width, runs parallel to the Atlantic coast and terminates in northern Gabon. Among the five major lithostratigraphical units of the Gabonese part of the West Congolian orogen, the West Congo Supergroup outcrops in the Nyanga synclinorium (Gérard 1958) and consists of the succession of several informal units. The 'Schisto-Calcaire Group' directly overlies the 'Niari Formation' (or 'Niari Tillite'), which, based on chronostratigraphic and sedimentological studies

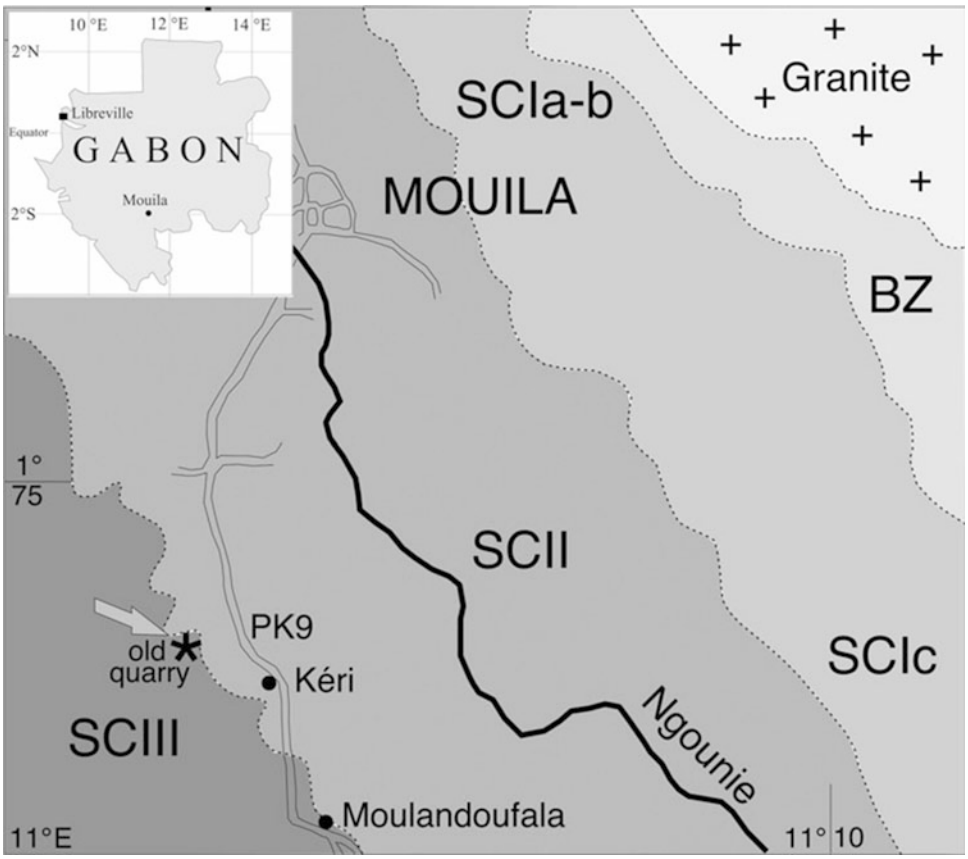

Fig. 5.1 General geological map of the studied area and location of Mouila city where the old Mouila quarry is situated, exposing the carbonate Neoproterozoic ('Nsc3' or 'SCIII') sampled for the study. Bz is for Bouenza 'Group', SCIa-b, SCIc and SCII for 'NSc1a-b, Nsc1c and Nsc2 formations of the Schisto-Calcaire Subgroup (modified from Thiéblemont et al. 2009; Préat et al. 2010)

in Namibia, has a proposed maximum age of 564 Ma (Saylor et al. 1998), and therefore likely correlates with the Gaskiers, or possibly another Ediacaran glaciation. However, the precise age of the formations of the West Congo Supergroup is still unknown.

The 'Schisto-Calcaire Subgroup' is predominantly a carbonate sequence with four formations ('Nsc1 to Nsc4'), and an overall maximum thickness of about 650 m. The lowermost three formations are calcareous to dolomitic shales with an uppermost sandy shale-siltstone unit with interbedded limestones. For our study, we collected fresh samples (standard thin sections and slabs were prepared from freshly cut samples after removing 2–3 cm from the outer surfaces) from formation Nsc3, which is exposed in the old Mouila quarry in South Gabon (Fig. 5.1).

5.2.1 Microfacies of the 'Nsc3 Formation'

In the old Mouila quarry, 20 m of thin to medium-bedded homogeneous dolo-mudstones interstratified with massive laminar peloidal and stromatolitic greyish dolomites are exposed (Figs. 5.2 and 5.3a,b). The rocks are partly silicified and contain stratiform black chert nodules, a few centimeters thick, between the beds and thin siliceous impregnations perfectly moulding the stromatolite laminae (Fig. 5.3c,d). Clays are not abundant and consist of subcentimetre-scale thicknesses. The stromatolites are hemispherical (height of 10–20 cm, lenghts up to 50 cm) and typically laterally linked (respectively LLH and SH, Logan et al. 1964, Fig. 5.3c,d). The facies are fine grained, mud-supported, greyish to slightly whitish and particularly homogeneous on the field (Fig. 5.3a,b).

Sixty samples were collected to ascertain the lithology and sedimentary features of formation Nsc1. Detailed imaging of the samples was performed using a JEOL Model JSM-6400 Scanning Electron Microscope (SEM) with a Pioneer Si–Li crystal X-ray detector (EDX) operated at a specific resolution of 138 eV. The samples were gold or carbon coated and mounted on metal stubs. The software used for spectral interpretation was a Voyager Version 3.5 from Thermo-Noran. High resolution images (1.2–3.0 nm at 15 and 1 kV, respectively) were further obtained with a JEOL JSM–7000F Field Emission Scanning Electron Microscope. Thin sections and rock slabs were sputter coated with gold-palladium and mounted on metal stubs.

The analyses enabled the recognition of 5 major 'diagenetic' dolomitic microfacies (MF1–5), whose succession (1–5) constitutes a standard sequence of shallowing-upward sedimentation and a corresponding increase in post-depositional diagenetic events related to the influence of hypersaline groundwaters in a sabkha-like environment

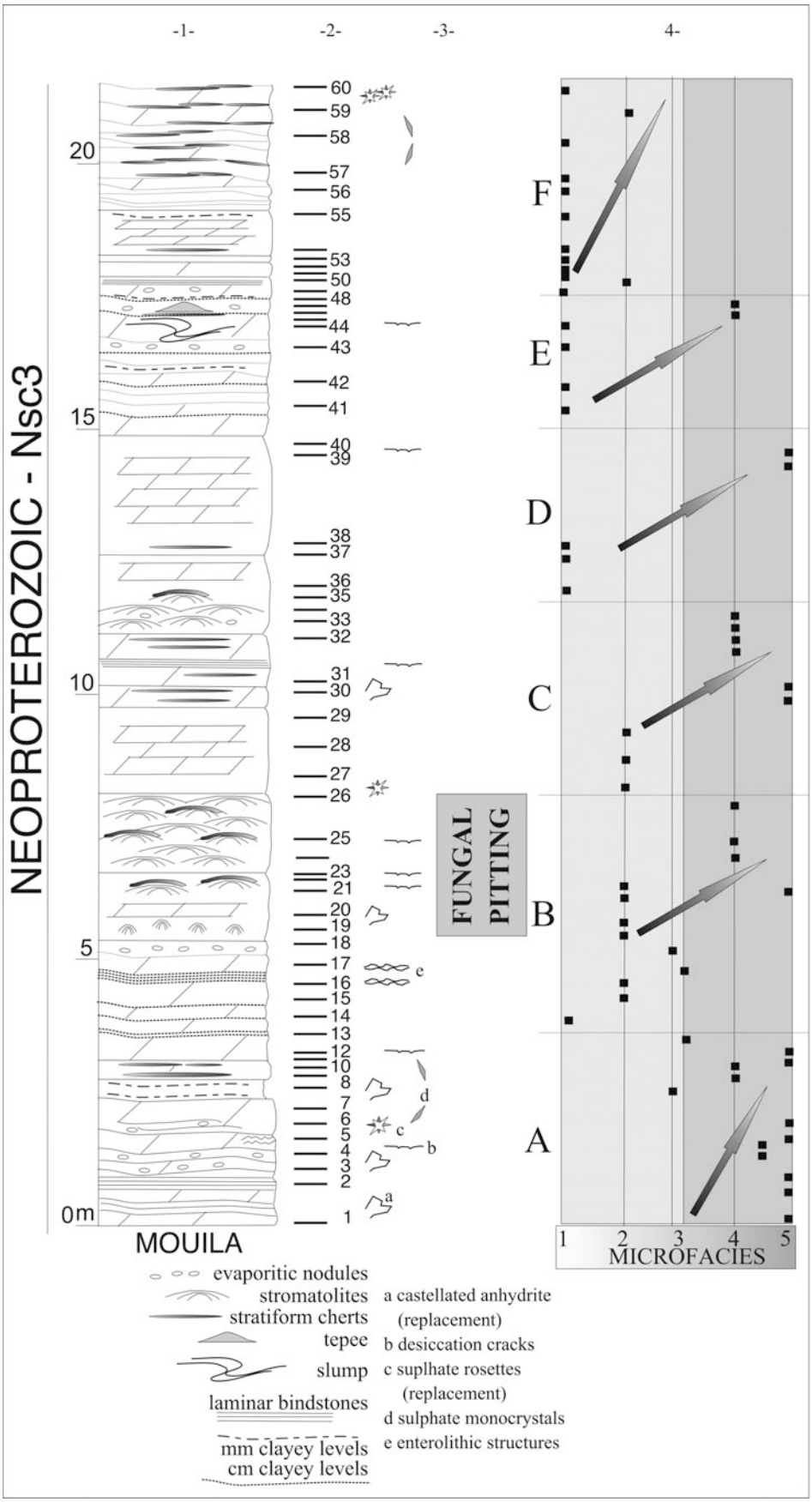

Fig. 5.2 Stratigraphy (column 1), lithology and sedimentary structures (column 2), position of sedimentological samples (column 3), position of samples illustrated on plates 1 and 2 (column 4) and lithological curve of the microfacies (column 5) of the Mouila quarry (Préat et al. 2010). The *arrows* inside column 5 indicate regressive shallowing-upward metric sequences (A–F), from shallow subtidal (microfacies 1 and 2) to supratidal and sabkha environments (microfacies 3–5). Samples 19 and 26 contain partly preserved cyanobacteria in the dolomicritic matrix (Fig. 5.4a) and well-preserved fungal hyphae in small-sized pits (Fig. 5.4b–d). The matrix of samples 22 and 23 is strongly replaced by homogeneous dolomicrosparitic crystals. See text for explanations and Fig. 5.3g, h

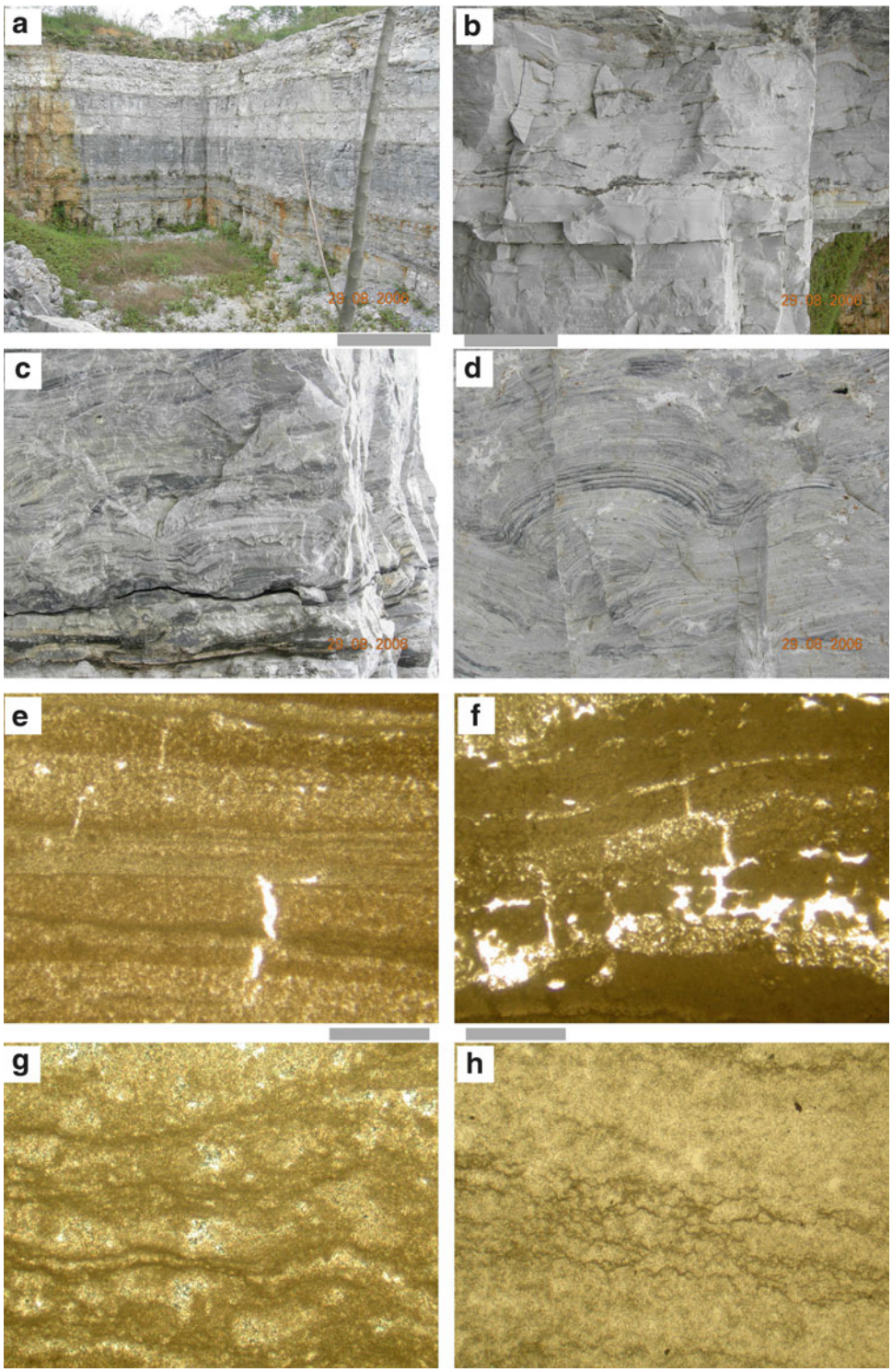

Fig. 5.3 (**a**) Mouila old quarry (South of Gabon). The picture shows the lower level of the series (10 m) belonging to the 'Nsc3' formation (Schisto-Calcaire Subgroup, Neoproterozoic). The level is composed of thin to medium-bedded homogeneous dolomudstones interstratified with stromatolitic greyish dolostones. The first massive stromatolitic layer occurs at 6 m from the base. The height of the front is 10 m (photo 1503/2006/ap). (**b**) Thin-bedded and laminated cyanobacterial greyish dolomudstones. Thin irregular undulating stratiform chert layers form slightly discontinuous *blackish* interstratified levels. Some 'ripples' are superimposed on slightly curved stromatolites. The *top* of the photograph is a thicker blackish chert level. *Lower part* of the massive stromatolitic layer (thickness of 60 cm), Mouila old quarry, Gabon (photo 1497/2006/ap). (**c**) Clusters of closely packed decimetric-scale greyish domal stromatolites interstratified with regular laminar (millimetric) thin cyanobacterial dolostones. Stratiform stromatolites are roughly parallel to layer orientation. Some flanking stromatolites are developed on sloped layers and are also interstratified with laminar dolostones. The base of the figure shows blackish chert levels. Other

(Fig. 5.2) (Préat et al. 2010). One of the primary facies consists of flat-laminated (Fig. 5.3b) to low domal stromatolite columns (Fig. 5.3c,d), the latter having laminae that form overlapping domes, with younger laminae truncating against older ones and leaving no intercolumn space. Laminae are produced by alternation of organic-rich and organic-poor horizons, with some individual laminae traceable over a few centimetres. The organic-rich horizons are generally richer in pyrite framboids (<1 μm up to 10 μm). The brighter layers contain micropeloidal micrite or clotted mudstone draping over dense mat layer. Mat constructors in thin section are poorly preserved morphologically (filamentous mat ghosts are present), but are still visible on the SEM despite the dolomitization process (Fig. 5.4b). In the outcrop, this 'cryptomicrobialite' is composed of submillimeter-scale white and gray micritic laminae couplets (Fig. 5.3e). Smooth flat laminated dolostone (Fig. 5.3f) associated with disrupted fenestral and crinkled fabrics are common. The latter typically exhibit near horizontal sheet-cracks associated with vertical and step-like thin mudcracks isolating micritic lumpy patches (Fig. 5.3f).

The major diagenetic alteration of the facies consists of a thin pervasive hypidiotopic dolomitization, probably related to episodes of anhydritization since sulphate microenterolithes developed inside the mats. Consequently, the former greyish microlaminar micritic sediment is progressively replaced by a relatively fine-grained homogeneous whitish dolo-microsparite, which may still contain thin discontinuous microbial mat relicts (Fig. 5.3g,h). At the beginning of the replacement process the dolomite is a mimetic fabric-preserving dolomite with crystal size varying between micrite and microsparite (<50 μm). As mentioned above, some evaporite minerals remain present in the matrix (i.e., not dolomitized) and consist of laths, rosette-like aggregates, enterolithic small nodules and castellated crystals (*sensu* Clark 1980) which often grow inside the mat levels. 'Elephant skin texture' with micropinnacles and net-like structures (Gerdes et al. 2000) are common in the facies associated with the stromatolitic layers. Silica is the last diagenetic phase observed.

5.2.2 Paleoenvironmental Interpretation

Micritic, millimeter-scale laminae interstratified with organic-rich thin horizons (benthic microbial mats, Fig. 5.4a) indicate initial deposition in a tidal-flat environment (Purser 1973; Hardie 1977; Sellwood 1986). The soft peloidal mud contains wavy and discontinuous lenticular laminae. Crinkled fenestral laminae (Fig. 5.3f), being either flat or domal, even (Fig. 5.3e) or pinching (Fig. 5.3f), are probably related to cyanobacterial mats. Despite strong diagenetic overprinting (microsparitization, dolomitization), slightly altered bacterial filaments are still observable by SEM imaging of the stromatolite laminae (sample MOU26, Fig. 5.4a).

The sediment laminae of the Mouila facies are typically disrupted by mudcracks and sheet-cracks a few millimeters to a few centimeters long associated with irregular small-sized fenestrae. Similar characteristics are observed today in the low 'algal' marshes fringing the ponds of channeled belts at Andros Island (Hardie and Ginsburg 1977), particularly along the backslope of the levees and the beach-ridge washovers where very shallow (millimeter range), closely spaced (around 1 cm) mudcracks are present. The cracking process may be quickly stopped by rapid growth of cyanobacterial colonies (microstromatolites) giving incomplete mudcracks as those present in Fig. 5.3f.

Sedimentological evidence also reveals that the Mouila series consists of a succession of plurimetric-thick shallowing-upward sequences which correspond to early diagenetic salinity cycles (Fig. 5.2, cycles A–F,) with well-developed upper parts related to subaerially exposed mudflats in a marginal marine sabkha. The cycles start with open marine subtidal-intertidal sedimentation in association with stromatolites (MF1 and MF2) and grade into

Fig. 5.3 (continued) discontinuous thinner silicified zones are present in the stromatolites (see Fig. 5.3d) and in the laminar dolostones. Massive stromatolitic layer (1 m thick), Mouila old quarry, Gabon (photo 1458/2006/ap). (**d**) Domal hemispherical stromatolites (LLH Logan's type, 1964) with very *thin blackish* chert layering. Stromatolitic *greyish* and *whitish* laminae are gently convex, without pronounced asymmetry in the domes. They are only interrupted when a slope is encountered. Massive stromatolitic layer, wide of the stromatolitic dome is 16 cm, Mouila old quarry, Gabon (photo 1467/2006/ap). (**e**) Smooth flat laminated dolostone composed of the alternation of millimetric fine-grained well-sorted peloidal laminar dolopackstone and thinner homogeneous dolomustone. The laminae are rather parallel at this scale of the microphotograph but pinch out laterally at at pluricentimetric scale. Small-sized vertical mudcracks cut several laminae. Sample MOU26, Mouila old quarry, Gabon (photo 0400/2006/ap). The sample has been taken in the domal stromatolite of Fig. 5.3c. (**f**) Crinkled fenestral laminar dolostone of the same type as Fig. 5.1e. The laminae are wavy, some contain sediment 'clots' or irregular peloids, particularly near the fenestral fabric. Sample MOU26, Mouila old quarry, Gabon (photo 0401/2006/ap). The sample has been taken in the domal stromatolite of Fig. 5.3c. (**g**) Irregularly dolomicrosparitized mudstone with remnants of thin layers of homogeneous blackish dolomudstone of the same type of those illustrated in Fig. 5.3e, f. The dolomicrospar is greyish and displays a patchy distribution, it contains slightly recrystallized dolomicrite matrix. Sample MOU22, Mouila old quarry, Gabon (photo 0417/2006/ap). (**h**) Strongly dolomicrosparitized mudstone with very thin uneven remnants of blackish dolomudstone. The dolomicrospar is coarser than in Fig. 5.3g and more whitish. Sample MOU23, Mouila old quarry, Gabon (photo 0409/2006/ap). Scale bars = 1 mm (**h**) and 400 μm (Fig. 5.3f, g)

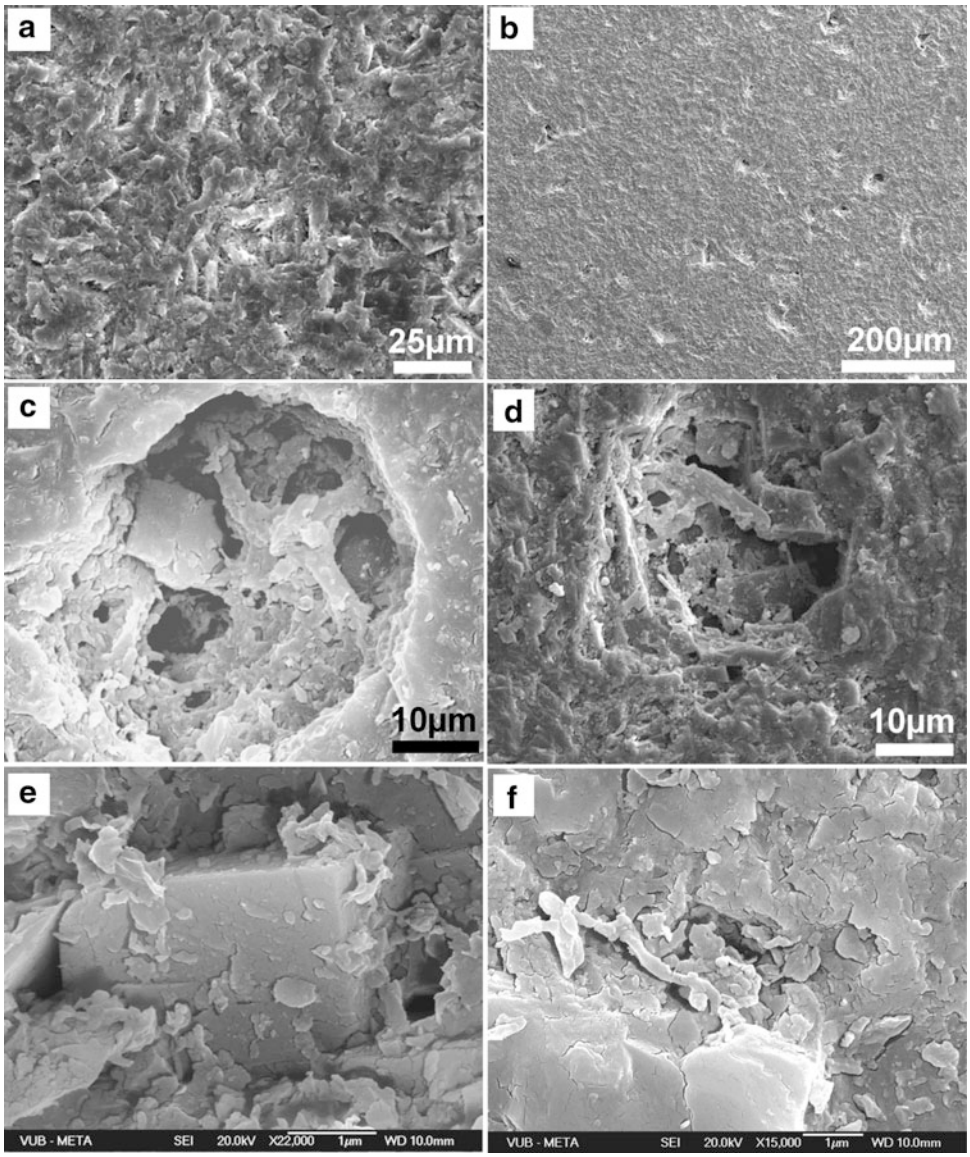

Fig. 5.4 (**a**) Filamentous dichotomous bacterial (probable cyanobacteria) ranging from 2 up to 5 µm in diameter. They are partly destroyed by a fine-grained dolomicropsar. The photograph has been taken in a homogeneous dolomudstone layer (see Fig. 5.3f). Sample MOU26, Mouila old quarry, Gabon (photo mou26-63/2007/ap). (**b**) Surface of sample MOU26 (*thin section*) under the SEM showing numerous inframillimetric irregular to subrounded pits or 'cavities'. Sample MOU26, Mouila old quarry, Gabon (photo mou26-8/2007/ap). The sample was taken in the domal stromatolite of Fig. 5.3c before any previous treatment (acid attack, coloration). (**c**) Small-sized (~30 µm) rounded pit in a dolomicrosparitized mudstone. The pit is filled with various microbial filaments forming a mesh containing well-crystallized minerals (see Fig. 5.3e). The filaments are slightly curved, some are dichotomous or rod-shaped, and the larger have diameters varying from 0.5 up to 1 µm. The dolomicrospar is irregular, varies in size between 1 and 3 µm and covers partly destroys the filaments. Thinner and shorter filaments (0.1–0.2 µm in diameter) are also present. Sample MOU19, Mouila old quarry, Gabon (photo mou19-17/2007/ap). (**d**) Small-sized (~25 µm) pit in a dolomicrosparitized mudstone (see Fig. 5.4a). Same filaments as previous figure with diameters ranging from 0.25 to 1 µm. Dolomicrospar is more regular and consists of small-sized (1–5 µm) well crystallized rhombs growing from a dolomicritic matrix. Thinner (0.1 or less micron in diameter) are associated with the larger filaments. They exibit a discrete *barrel-shaped cells*. Some filaments are engulfed in the dolomicrospar. Sample MOU26, Mouila old quarry, Gabon (photo mou26-20/2007/ap). (**e**) Quadratic dolomite crystal probably derived from a calcium oxalate crystal associated with a few irregular microbial filaments (see upper corners of the crystal) with diameters around 0.1 µm. The crystal is long of 2.5 µm and has grown in a pit similar to those illustrated in Fig. 5.4b. (**f**) Thin filament with *septate* appearance similar to hyphae and diameters <1.0 µm likely enveloped by EPS material. Other thicker filaments (flattened?) appear well-embedded in the pit walls. Sample MOU19, Mouila old quarry, Gabon (photo mou19-21/2007/ap)

evaporitic supratidal conditions or subaerial exposition (MF–MF5) with progressive replacement of primary evaporitic minerals by dolomite (dolomicrosparite). The diagenetically altered upper parts of the cycles are related to subaqueous deposition of muds associated with desiccation and/or intrasediment precipitation of evaporitic

minerals from groundwater brines, similar to some modern sabkha evaporites. Samples MOU19, 22 and 23 (Fig. 5.2) are strongly affected by evaporite brines leading to dolo-microsparitization of the microenterolithes and sample MOU26 is characterized by desiccation (Figs. 5.2 and 5.3e, f). These samples containing "fungi" (samples MOU19, 23 and 26) come from the upper part of such a diagenetic salinity cycle overprinted on a stromatolitic layer (cycle A, MOU19) and cycle B, MOU22, 23, 26 Fig. 5.2) (Préat et al. 2010, 2011a, b).

5.3 Detailed Petrography of Nsc3

5.3.1 Diagenetic Alteration

Both dolomicrite and dolomicrosparite replace (at an infra-millimeter-scale) the microbial laminae and developed progressively from the cyanobacteria which are partly or totally mineral-enveloped and still recognizable: they form a 3D-network, some are dichotomic, the average diameter is between 2–5 μm and their minimal length is 20 μm (Fig. 5.4a). Dolomite crystals are greyish (abundant micritic inclusions), xenototopic to hypidiotopic and approach sizes up to 50 μm. Larger whitish hypidiotopic crystals (50–100 μm) are associated with the replacement of former sulfate crystals and irregular fenestrae. The association of fine-grained dolomite with mudcracks and sheet-cracks (disrupted flat laminar lamination), together with their very fine grain-size and the presence of former sulfates, suggest that dolomite is a secondary mineral phase, most likely precipitated from hypersaline waters during the dry season.

Petrographic and SEM study reveal abundant subrounded (circular to oval-shaped) and irregular pits (quasi-rectangular) in the first stromatolitic level (samples MOU19 and MOU26, Figs. 5.2 and 5.4b). They range between 5 and 50 μm and are spatially arranged into either single pits or a network pattern. The latter is formed from boundary-connected subrounded-rounded pits that form a honeycomb or alveolar structure containing both colonizing fungal material and neominerals (see Sect. 4.1 below). Generally, single pits show three major features. The first is the presence of an elevated mineral "collar" or ring (originally probably Ca- or Mg-oxalates) around the pits' circumference that is composed of authigenic minerals. The second is the deposition of authigenic minerals inside the pits in a process which we are tempted to call "nesting". The minerals are dolomite in the form of rhombohedra (Fig. 5.4c,d), but also as quadratic crystals possibly related to former oxalates (Fig. 5.4e). The third, as discussed in the section below, is the colonization of the pits by invading fungal hyphae. Indeed, it is our contention that the pits are dissolution cavities related to fungal colonization of the original mineral substrate.

The colonizing microbes display various morphologies, more irregular than the ones of the cyanobacteria seen in the matrix, with non-septate (Fig. 5.4c) or septate-like (Fig. 5.4f) thin filaments similar to hyphae, and diameters <1.0 μm. Other filaments are more regular and have diameters varying between 0.25 to 1.0 μm (Fig. 5.4c). The filaments are associated and engulfed with what we presume to be fossilized EPS material (Figs. 5.4c–f and 5.5a,b). Some spherical bodies (diameter around 1.0 μm) are visibly adhering to the fossilized EPS (Fig. 5.5c–d). These spheres are richly encrusted with sub-micron sized rounded crystals that collectively yield the framboidal shapes characteristic for authigenic pyrite. However, microprobe analyses reveal that the spheres are entirely dolomite in composition. These spheres could represent fungal spores encrusted with mineral crystals. A similar observation has also been made under laboratory conditions (Kolo and Claeys 2005). The EPS is systematically desiccated (Figs. 5.4c–e and 5.5a–c) yielding strands reminiscent of actual microbial filaments. Very fine (<1 μm) aggregates of minerals or clusters adhering to the strands are frequently observed in the cavities (Fig. 5.4c–f).

5.3.2 Evidence of Fungal Colonization

The probable 'dolomitic' spores, the dolomitic prismatic quadratic and tetragonal crystals, the clusters of very fine crystals along the filaments and on the former larger crystals inside the cavities and the abundance of the thin filaments (<1.0 μm in diameters) in the pits suggest that the pits were formed through the activity of ancient fungi. Figures 5.6a–d show completely mineralized and well embedded forms in the rock matrix that can be attributed to fungal vegetative parts such as sporangia, sporangiophores and hyphae. Careful study of these images reveals a dense fungal colonization of the sediments, especially as shown in Fig. 5.6c–e. In Fig. 5.6e, f several individual fungal sporangia and sporangiophores can be clearly seen. The black color of fungal parts is attributed to organic content. The low contrast in the backscattered image (Fig. 5.6f) emphasizes the embedding of the fungal forms within the matrix and the uniform elemental composition. On close examination, the blackish sporangial area in the lower-mid part of Fig. 5.6e reveals that it is actually harboring three superimposed sporangial bodies that make intersecting circles. The lower one of these circles shows very fine and continous zig-zag wavy ornamentation likely representing the ancient ornamental spines or ridges at the perimeter of the sporangial wall. These are comparable to present day spine ornamentation on the sporangia of some Mucorales fungi (Alexopoulos and Mims 1979; Moore-Landecker 1991).

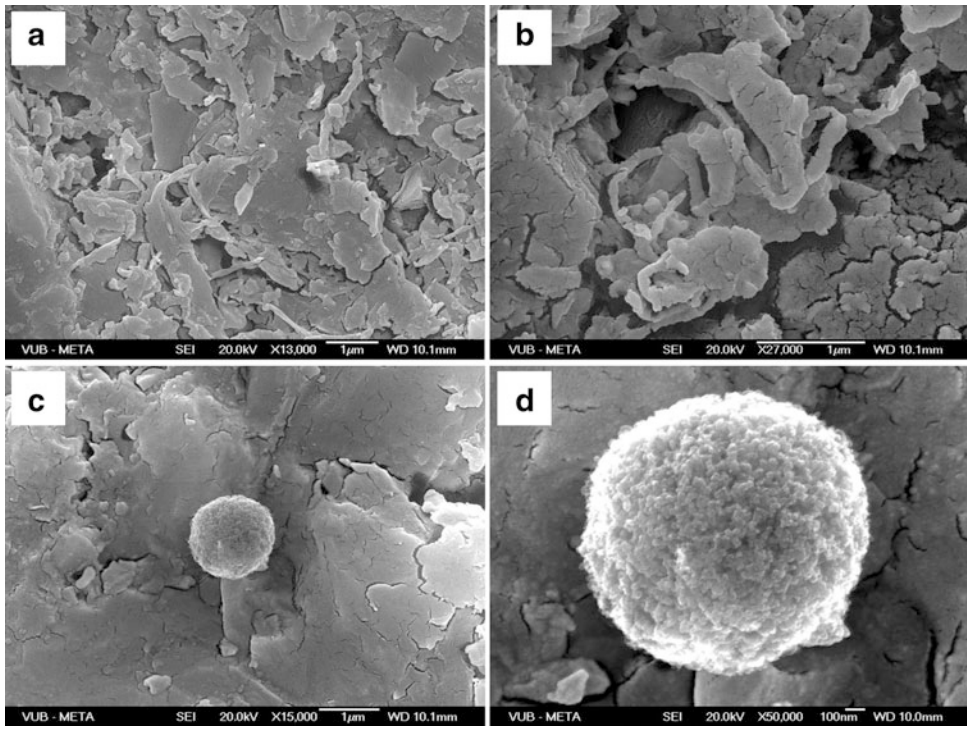

Fig. 5.5 (**a**) Very small-sized curved filaments (diameters around 0.1–0.2 μm) irregular embedded in platelet-like anhedral dolomite crystals (possibly former EPS substances). (**b**) Irregular polygonal networks of microcracks are omnipresent on the dolomite as well on the filaments. Sample MOU19, Mouila old quarry, Gabon (photo mou19-40/2007/ap). (**c**, **d**) Dolomitic sphere (diameter of 1 μm) inside platelet-like dolomicrospar with irregular microcracks. The *sphere* is composed of subrounded microcrystals of dolomite (10 nm in diameter, Fig. 5.5d). Sample MOU19, Mouila old quarry, Gabon (photo mou19-36 and 33 respectively/2007/ap). SEM photomicrographs. Bar scale: as indicated

Interestingly, some specific features of fossilized reproduction parts of fungi can be observed also. Figure 5.7a shows the remains of sporangial forms connected to their sporangiophores, and the black protrusions to the right suggest a typical form of spore dispersion. A second smaller sporangium lies next to the first structure. The first sporangium reveals two concentric circles separated by about a 8–10 μm thick zone. The inner circle is visibly continuous (diameter ~30 μm) and joins the sporangiophore. This structure and configuration actually reveal a fungal columella. Furthermore, Fig. 5.7b shows a richly colonized substrate (not all traces shown) where an external black perimeter of the sporangium suggests the sporiferous region of the sporangium with a probable attached spore mass. The traces of the ancient fungal parts are sometimes outlined by the dissolution figures, which relates the visible pitting on the Neoproterozoic substrates, at least in these instances, to fungal activity. Figure 5.7c shows another fungal-related shape and setting where possible sexual reproduction organs involving the formation of a zygosporangium and suspensors are observed. They display an anatomical morphology comparable to modern fungal sexual reproductive cycle and the production of zygosporangia, zygospores and suspensors, e.g., in the Zygomycetes (Alexopoulos and Mims 1979; Moore-Landecker 1991; Kendrick 2000).

A negative and enhanced image (Fig. 5.7d) of the above reveals the well-defined and preserved morphology and contours of these fungal structures that undoubtly appear well-embedded in the mineral matrix of the dolomitic substrate. This strongly suggests a pre-lithification synsedimentary process and early diagenesis. Moreover, these fungal structures are very similar to fungal parts retrieved from the Late Riphean Neryuenskaya Formation of southeastern Siberia (Hermann and Podkovyrov 2006), which represent the oldest reported fossil fungi.

Although the poor preservation caused by dolomitization and per-mineralization of fungal relicts do not allow for more detailed descriptions, and did not allow for extraction, the well-contoured fungal features, substrate dissolution, pit forms and colonization when compared with modern fungi (e.g. Mucorales), and their patterns of colonization and interaction with mineral surfaces, especially carbonates (Kolo and Claeys 2005; Kolo et al. 2007), nonetheless suggests strong similarities between modern and ancient fungi.

5.4 Neoproterozoic and Modern Fungal Diagenesis: Analogous Patterns

We have attempted to experimentally demonstrate (detailed experimental procedure *in* Kolo and Claeys 2005; Kolo et al. 2007) that fungal interaction with dolomite crystals produce characteristic colonization patterns, dissolution, pitting, and neomineral formation "nesting" as observed in our Neoproterozoic strata. For the experimental work, thin

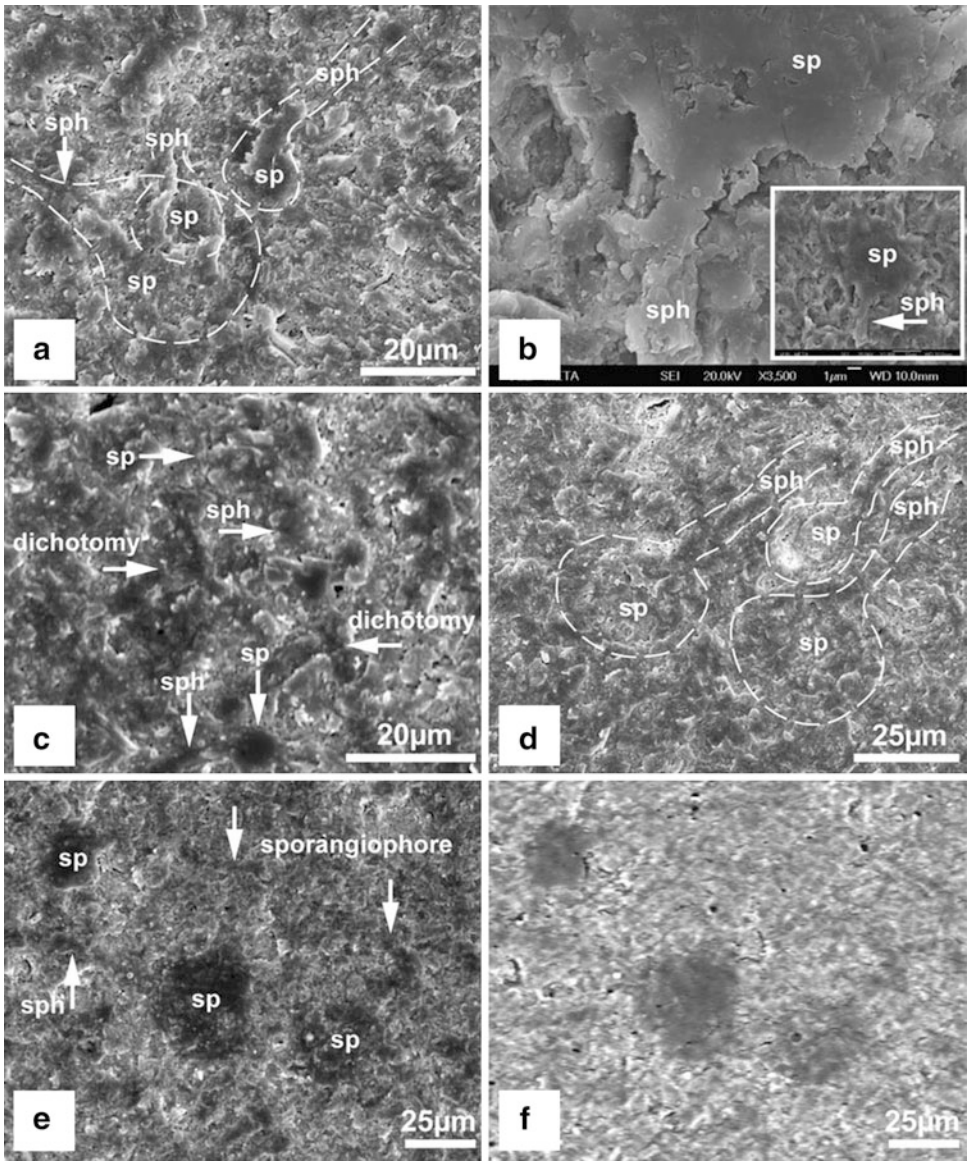

Fig. 5.6 Permineralized embedded relicts and ghost traces of fungal remains in the Neoproterozoic section of Mouila, Gabon depicting typical fungal structures that colonized the substrates. Pictures are from samples MOU26 (Fig. 5.6a, c, d, mou26-15, 26-23, 26-9/2007/ap), MOU 19 (Fig. 5.6b, 19-2/2007/ap) and MOU22 (Fig. 5.6e, f, 22-23, 22-24/2007/ap) (**a**) Per-mineralized (now dolomitic) sporangi(a)um (sp) appear attached to their sporangiophores (sph). In the *lower-left* appear two superposed sporangia. The *dashed lines* contour the visible morphology of these forms. (**b**) A visible per-mineralized single sporangium (sp) attached to its sporangiophore (sph). The inset figure shows the entire contour of this reproduction structure and its complete embedding in the rock matrix. (**c**) Various sporangia and sporangiophores showing blackish color probably related to organic content. In the lower part of the figure is a typical sporangial and sporangiophore shape of fungi. Dichotomy is also visible. (**d**) Here, together with Fig. 5.6a–c, the pits' shapes can be at least partly related to fungal remains, especially the sporangia from where the oval and circular shapes of pits are seemingly inherited. The detailed scrutiny of these figures reveals the rich colonization of these deposits by fungi. (**e**) Normal SEM image showing similar fungal remains compared to secondary backscattered image. (**f**) where the traces of the fungal remains are deeply imprinted in the substrates

sections (4 × 2 × 0.5 cm) and rock slabs from Carboniferous dolomites of the Terwagne Formation (Viséan, Bocahut quarry at Avesnes-sur-Helpe, northern France, in Mamet and Préat 2005) were used as substrates for fungal interaction. All samples were examined at the end of the experimental work by FE-SEM, SEM and EDX.

5.4.1 Honeycomb Dissolution Pattern

The Neoproterozoic thin sections show secondary porosity that is developed after dolomite crystal dissolution. Rhombic and quadratic pore spaces are still discernable in many instances (Fig. 5.8a) and are typically arranged in a

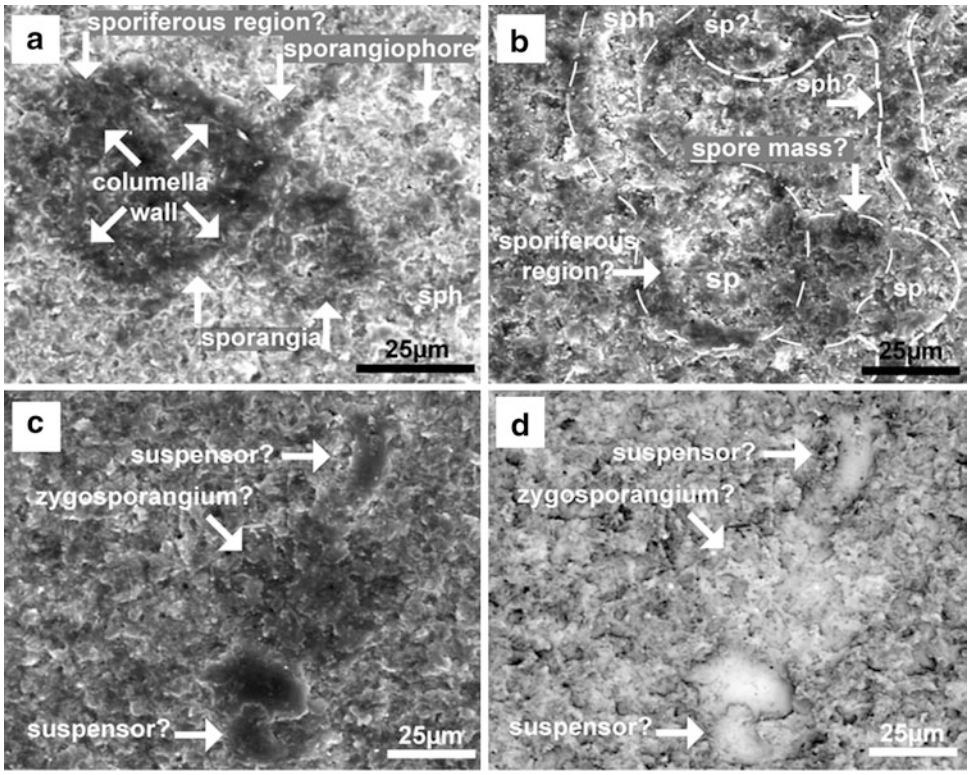

Fig. 5.7 SEM photomicrographs of relicts of fungal structures from Neoproterozoic section of Mouila quarry, Gabon. Sp = sporangi(a)um, sph = sporangiophore. Bar scale as indicated. Images are from samples MOU22 (Fig. 5.7a–d 22-20, 22-16, 22-18, 22-17/2007/ap) (**a**) Fungal remains showing sporangia (*black rounded bodies*), sporangiophores (sph), and a probable sporiferous region. In the larger sporangium are seen two concentric perimeters, the internal one (delineated by *white arrows*) depicts the columella. (**b**) Richly colonized substrate (not all traces shown) where sporangia are showing an external black perimeter depicting a sporiferous region and a probable spore mass attached to it. The traces of the ancient fungi are clearly outlined by the later dissolution diagenesis. (**c**) The visible shapes, compared to modern and ancient fungal analogues (e.g. *in*: Alexopoulos and Mims 1979; Hermann and Podkovyrov 2006), depict zygosporangium and suspensors. (**d**) For further demonstration, here is an artificially enhanced negative image from Fig. 5.7c. The permineralized structures shown in Fig. 5.7c are visibly outlined. Note how well the structures are immersed in the matrix, indicating a syn-sedimentary process

honeycomb pattern. The pore space boundaries contouring the shape of dissolved crystals have a filamentous appearance with fine crystal aggregations (Fig. 5.8a). This arrangement strongly resembles the pattern of interaction of modern fungi with Carboniferous dolomites (Fig. 5.8b). Experimentally, fungal invasion of carbonate substrata have been shown to selectively occur by hyphal penetration along grain boundaries (Sterflinger 2000; Kolo et al. 2007). This stage is followed by active microbial dissolution of the crystals through organic acid generation, creating hollow dolomite crystals or whole rhombic-quadratic and roundish pore spaces with fungal hyphae as boundaries and authigenic mineral deposition (biominerals such as Ca- and Mg-oxalates: weddelite, whewellite and glushinskite). These hollow dolomite crystals, where only boundaries are preserved, are diagenetically different from dolomite crystals with hollow centres and preserved rims (Vahrenkamp and Swart 1994; Feldmann and McKenzie 1997; Jones 2005) that may have precipitated on minute particles or metastable material andwas subsequently dissolved or from bacterially-formed dumbell-shaped hollow-core dolomite crystals (Cavagna et al. 1999).

5.4.2 Intracavity Biomineralization in Natural and Experimentally-Weathered Dolomites

Figure 5.9a shows a circular pit surrounded by a visible elevated mineral "collar" that was also observed in some thin sections of Neoproterozoic strata. Tiny crystals and also per-mineralized filaments litter the interior and exterior of the pit. The mineral "collar" consists of a mixture of per-mineralized filamentous material (probably with EPS material) and attached crystals. Similar diagenetic features (Fig. 5.9b) comprising pits formed by dissolution of

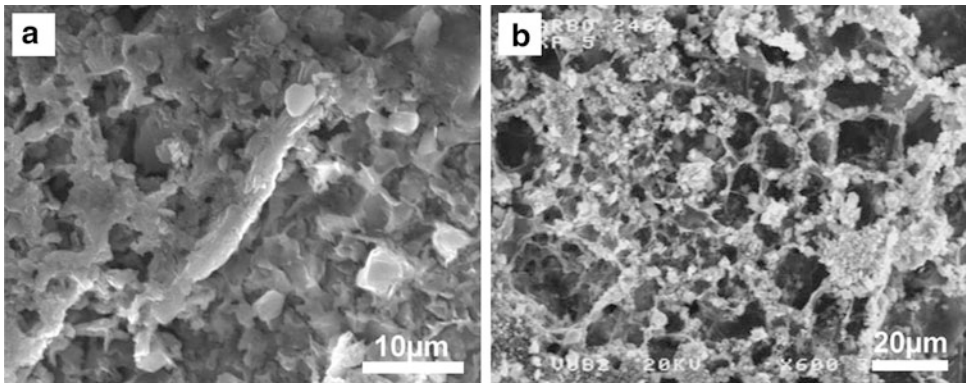

Fig. 5.8 SEM photomicrographs from samples MOU26 (Fig. 5.8a mou26-2/2006/ap) and sample carb246A, showing comparative honeycomb-alveolar structures produced by fungi on dolomitic substrates. Bar scale as indicated. (**a**) An ancient and naturally produced one from the Neoproterozoic of Mouila quarry, Gabon and (**b**) an experimentally produced structure from the Carboniferous of the Bocahut quarry in France. Both figures share common features, such as quadratic-rhombic pore space after the dissolution of dolomite crystals and the formation of a filamentous-EPS mat cover on old crystal boundaries associated with new crystal deposition on those boundaries, suggesting a similar colonization pattern and diagenetic process. In Fig. 5.8a the original fungal material (filaments and EPS) are all permineralized but the old honeycomb-alveolar structure is still well preserved

dolomite crystals, an elevated mineral "collar" composed of mineral authigenesis (here Ca-oxalates—weddellite and whewellite), fungal hyphae and EPS material lining the pits were experimentally produced by fungal interaction with a dolomite substrate, indicating these diagenetic features are a characteristic of fungal interaction with carbonate substrata and generally also a part of the honeycomb structures demonstrated above. Figures 5.9c, d reveal more details on the above-mentioned similarities. In both cases, the filaments are occasionally encrusted with fine crystals (Fig. 5.9c) and usually form a lining on the pit wall. Fungal hyphae are known to form envelopes of Ca-oxalates crystals that partially or completely engulf the hyphae especially under Ca-rich conditions (Gadd 1999; Verrecchia 2000; Kolo and Claeys 2005). This crystal adherence to fungal hyphae is also visible in both cases.

"Nesting" is a term we use here to describe the deposition of fungally produced biominerals, mainly Ca–Mg-oxalates or even calcite, in the partially to totally dissolved crystals of dolomite substrata (Fig. 5.9e, f) following fungal colonization and growth. In our experiments, these biominerals are much finer (1–3 µm) than the original substrate crystal size and typically are represented by various forms of Ca-oxalates: prismatic, tetragonal bipyramidal, and rhombic (Fig. 5.9f). Such fine crystals are also observed in the Neoproterozoic pits (Fig. 5.9e). The formation of these metal-oxalates is largely attributed to the reaction of oxalic acid, excreted by fungi, and the high availability of Ca^{2+} and Mg^{2+} in the growth environment (Gadd 1999).

5.5 Discussion

5.5.1 Neoproterozoic-Aged Colonization and Weathering

The Neoproterozoic carbonate stromatolites of the Mouila series were originally composed of a magnesian micritic mud colonized by benthic cyanobacterial mats in a shallow tidal depositional system. Then, through a combination of microbially-induced biomineralization of fine- to medium-grained dolomicrospar, coupled with copious EPS excretion, the original muddy sediment was transformed into domal stromatolites, similar to those occurring today in evaporitic carbonate sabkha-like environments (Walter 1976; Grotzinger and Knoll 1999). These microbialites seemed to have resisted erosion as evident by the preservation of the overall morphology and internal features of the stromatolites (see below). As suggested by the typical shallowing-upward sequences, this semi-lithified to progressively well-lithified sediment experienced periodic or episodic desiccation (as revealed by a 'polygonal pattern of cracks' of the mud in thin sections and the EPS under the SEM) coupled with evaporitic salty brine invasion leading to gypsum and other evaporitic minerals being interstratified within the mats. Cyanobacteria were progressively destroyed and cementation was the dominant process. During this period of subaerial conditions, fungi were able to colonize the substrate and drive carbonate diagenesis. The most striking result of their activity was the formation of the circular-oval-shaped pits in

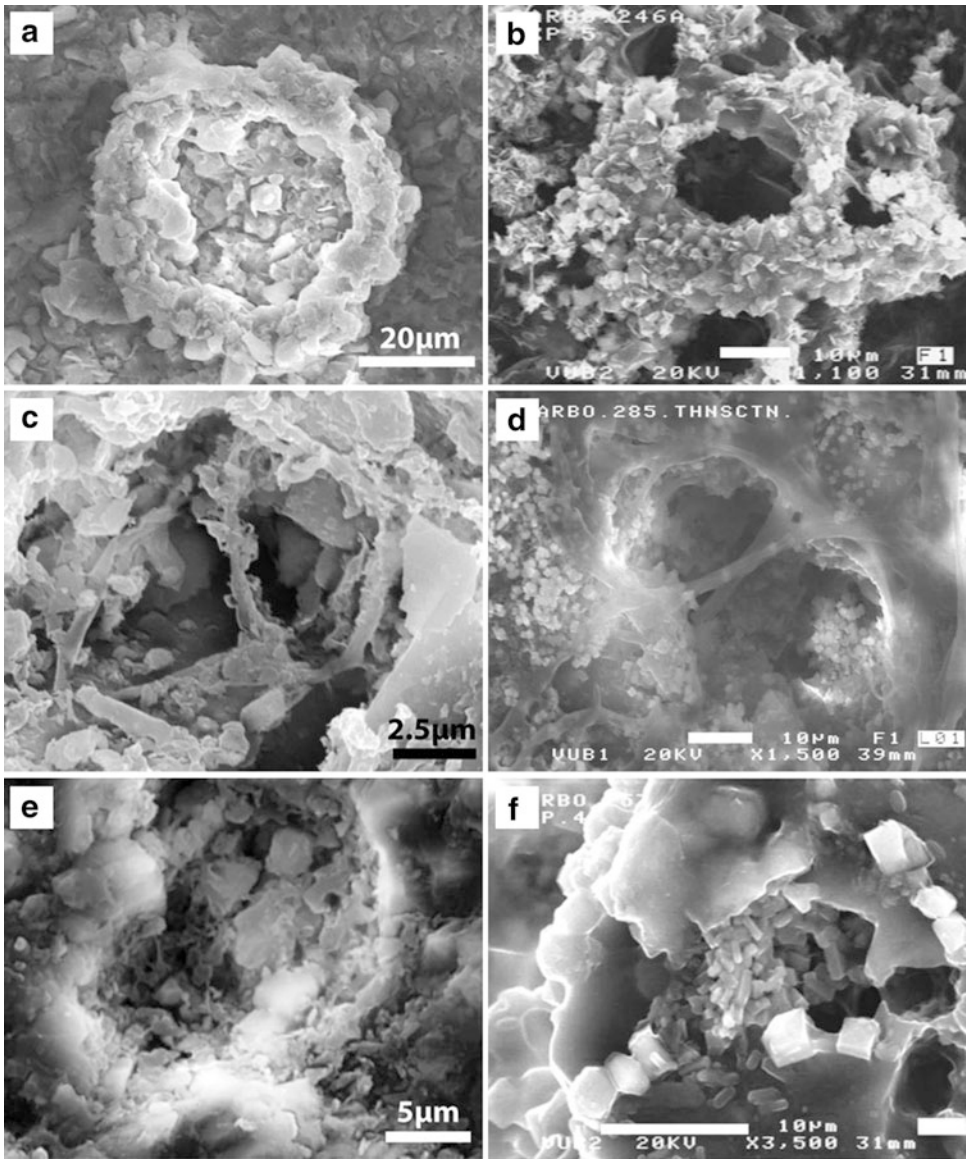

Fig. 5.9 Images showing comparative patterns of fungally produced mineral deposition "nesting" and colonization of pits as fossil and permineralized fungal relicts in the Neoproterozoic of Mouila section, Gabon (Fig. 5.9a,c,e) and of pits from *in vitro* experiments (Fig. 5.9b,d, f) on Carboniferous dolomite of the Bocahut quarry in France. Pictures are from samples MOU22 (Figure a, mou22-22/2006/ap), MOU 19 (Fig. 5.9c,e, 19-17, 19-38/2006/ap) and samples carb246A, 285 and 257 (Fig. 5.9a,b). Elevated mineral "collar" formation surrounding a pit. In (**a**) the pit appears filled with mineral crystals (dolomite) and the mineral collar is a mixture of crystals and per-mineralized filaments. In (**b**) the deep pit reveals similar mixture of neominerals (here Ca- and Mg-oxalates) and fungal hyphae. (Fig. 5.9c, d) Colonization pattern of formed pits by fungi appears similar especially the lining of inner walls of the pits. Note how the filaments' surface in (**c**) is rough and show many blebs and attachments. These are crystal aggregates adhering to their surface, a typical fungal phenomenon as is also shown in Fig. 5.9a. In (**d**) the colonizing fungi have already produced a large quantity of crystals inside and outside the pit (**e**, **f**) Showing further the "nesting" of minerals by fungal interaction with the substrates. In Fig. 5.9e fine crystals and filaments are littering the pit's bottom as well as the walls, while in Fig. 5.9f a typical pit made in a dolomite crystal is filled by fungally bio-mineralized prismatic and bi-pyramidal crystals of the mineral weddellite

the stromatolitic levels. The fungal relicts are well-embedded in the rock matrix and show homogenous early diagenetic character which indicates their penecontemporaneous nature with lithification, i.e., the Neoproterozoic.

There are several lines of evidence that support our contention that the pits formed while the sediment was already lithified and that this rock constituted a good substrate for fungal colonization:

1. The pits are hosted in a substrate formed from uncompacted sediment. The grains (flat pebbles, microbreccia, lumps, and aggregates) and the fenestral cavities are undeformed, and they do not exhibit any

interpenetration, because the pseudomorphs of sulfates or the microenterolithic levels have not collapsed. These replacements were probably formed nondisplacively in an enclosed volume of lithifying muddy sediment. Dolomite and also fine- to coarse-grained silica have completely replaced these original voids, thus maintaining their original shapes without deformation. The process was probably rapid, as no mechanical compaction and fracturing are observed. This early replacement-cementation (dolomicrospar) prevented late fracturation due to overpressuring in response to burial.

2. The mudcracks and sheet-cracks are well preserved, undeformed and filled with a dolomicrospar (and sometimes silica) having the same size (generally very-fine to fine-grained) as the dolomicrospar that replaced the primary carbonate mud. Boundaries separating peloid and muddy laminae are quite sharp and of constant thickness inside a particular laminar structure. No interpenetration of the different laminae is observed. Detailed fabric preservation of primary cracks suggests that dolomitization and silicification occurred early in the diagenetic history; they do not cross the cracks.
3. Evaporite facies display micro-slumped or contortion structures without any signs of compaction. The tiny contorted levels are folded, keeping their uniform original thickness (<200 μm for the thinnest).
4. The pits and fungi are confined to the same stratigraphic levels in a stromatolite horizon. In the field, the laminar structure consists of irregular bands and lenses of dark and light carbonate mudstone. The bands constitute sets with uniform thickness.
5. The spheres attributed to spores are dolomitized at a nanoscale level and embedded in the dolomicrospartic matrix.
6. The pits are invaded by thin hyphae associated at a very small scale (<100 μm) with former quadratic crystals which were probably primary oxalates (identical to our experiments). Those oxalates were then dolomitized through either the cycling of dolo-microspar or simply via interaction with near-coeval seawater or seawater-derived fluids.
7. Excellent fabric retention of highly-soluble evaporate phases (rosettes, swallow-tails, laths, microenterolithes, and nodules) during dolomitization indicate that dolomitization had occurred under hypersaline conditions. These conditions are also suggested by ^{18}O enrichment of the facies constituting the upper part of the shallowing-upward salinity sequences where the fungi developed. Oxygen isotopes ($\delta^{18}O$) (Préat et al. 2010), have values ranging from −5.1 to −1.3 ‰, recording stabilization in normal Neoproterozoic marine water (Veizer et al. 1992). Lighter values indicate continued evaporation and upwards percolation of underlying pore waters, ruling out an increase in temperature (during burial) and an early or late influence of meteoric fluids. In this context, late-stage diagenetic alteration resulting from large-scale convection of marine, meteoric or hydrothermal waters during burial can be dismissed. The dolomicrospar is therefore neomorphic and replaced the original fine-grained (dolo)micrite without a dissolution phase.

Collectively, these points lead one to infer that the primary carbonate muds were rapidly lithified by dolomitization associated with evaporitive marine or coeval marine waters. Under such conditions, fungi were able to inhabit this stressful environment and subsequently played an important role in the pit formation in specific or particular interstratified levels (here a stromatolite layer).

5.5.2 Fungal Colonization and the Pit Formation Hypothesis

The different depth levels of these the fungally-generated solution pits suggest a progressive process of pit formation through incipient, moderate and advanced pitting stages (Fig. 5.10a–d), possibly caused by different stages of microbial colonization-diagenesis. The incipient pit stage (Fig. 5.10a, b) has a shallow quasi-circular/oval form, visibly corresponding to a bioweathered, fragmented, micropitted, and decolorized original mineral surface compared to the surroundings where some fine-grained authigenic minerals had started to precipitate. Interestingly, some incipient pits visibly show fungal form morphology (Fig. 5.10a) that suggests a sporangium and sporangiophore relicts. This morphological resemblance between fungal parts and pits' leads us to assume a cause and effect process.

In moderately developed pits, colonization by fungal forms and mineral authigenesis can already be observed (Fig. 5.10c) relating the two processes and suggesting an interaction of fungally induced biochemical and biomechanical factors with the mineral surface. The circular/oval shape of the pits suggests therefore an inherited form after the fungal parts (e.g., sporangia, as depicted by Fig. 5.10a) or by selective fungal attack on certain sites of weakness on the mineral surface (e.g., Fig. 5.10c, grain boundaries giving rise to irregular pit shapes). Selective fungal attack that produced alveolar-type mineral structure and pitting has already been shown to occur with dolomite and limestone (Kolo et al. 2007).

At the advanced stage, the pits have clear 3-D forms, display visible inner walls, depth and variable diameters (Fig. 5.10d). Inside the pits, a dense network of colonizing fungal hyphae are interwoven with the pit's inner walls as well as the bottom which was coated with EPS (Fig. 5.10d).

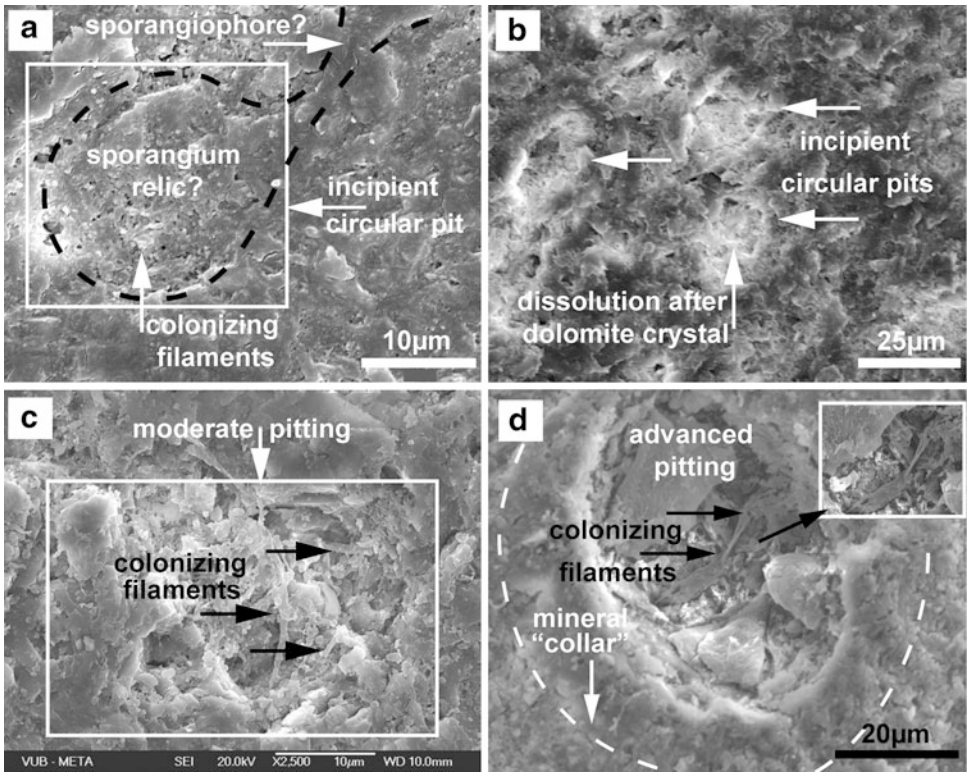

Fig. 5.10 Images showing three stages of pit formation in the Neoproterozoic section of Mouila quarry, Gabon. SEM and FE-SEM photomicrographs (from thin sections). Bar scale as indicated. *Black* and *white strokes* are for contrast only. Pictures are from samples MOU26 (Fig. 5.10a, mou26-14/2007/ap) and MOU 19 (Fig. 5.10b,c, d, mou19-7, 19-14, 19-49/2007/ap). (**a**) Incipient pitting with quasi circular shape displaying many small pits (*black spots* <1µm) and fragmented surface lower than the surrounding. The surface is bioweathered. In the centre of the pit, very small colonizing filaments (~1 µm) can be observed. The whole pit displays the form of a fungal sporangium attached to its sporangiophore. (**b**) Shows similar several incipient pits. The *lighter colored* areas are characteristic of pit formation. Interestingly, is also visible the slightly elevated mineral "collar" of the pits. (**c**) Moderately formed pit, with shallow depth but visibly deeper than the incipient ones. In this stage, colonization by microbial filaments (fungal?) is important and associated with small neomineral formation (*white crystal* aggregates in the centre). The colonizing filaments occupy the centre of the pit as well as the border of pit wall. (**d**) The advanced pitting stage creates well-developed pits with well-defined contours, formation of elevated mineral "collar" around the pit as well as mineral deposition inside the pit, and rich colonization by microbial filaments associated sometimes with polysaccharides film

Sometimes, these fungal hyphae form a 'lining' to the inner walls. Authigenic minerals related to fungal activity litter the pits and are visibly attached to fungal material as well. The latter minerals are distinguishable by their light color and inherited crystal forms. Originally, the minerals, now dolomitic, were probably Ca- or Mg-oxalates (weddellite, whewellite or glushinskite). The spatial distribution of these mineral forms is visibly restricted to encrusting the fungal hyphae at the inside of the pit and to the "collar" area surrounding the pit. This limited distribution is consistent with fungal activity. Furthermore, the colonization of the pits by fungi displays a complex pattern (Fig. 5.10d and inset) that highlights the invasive behavior of fungal hyphae into the pit walls and the mineral matrix that resulted in micro-fragmentation of the pit's wall through both mechanical dislocation and chemical dissolution in addition to mineral precipitation.

The mechanisms underpining the three-stages of pit formation are schematically represented by two scenarios (Fig. 5.11) that could have worked separately or in combination. The first mechanistic scenario involves fungal colonization of the Neoproterozoic substrate through hyphae-stolons and rhizoids invasion of the semi-lithified sediment surface, penetrating along grain boundaries. This process would have resulted in grain dissolution by fungal organic acids exudates (mainly oxalic), increasing the pore space and, with continuing colonization, development of pits with authgenic minerals precipitating on their external perimeter and within their inner walls. These pits themselves become the target of new invasion by exploratory fungal hyphae. This scenario is shown to occur in experimental studies (Kolo et al. 2007). In a calcium-magnesium rich environment, the formation of oxalate biominerals (e.g. weddelite whewellite and glushinskite) would have been

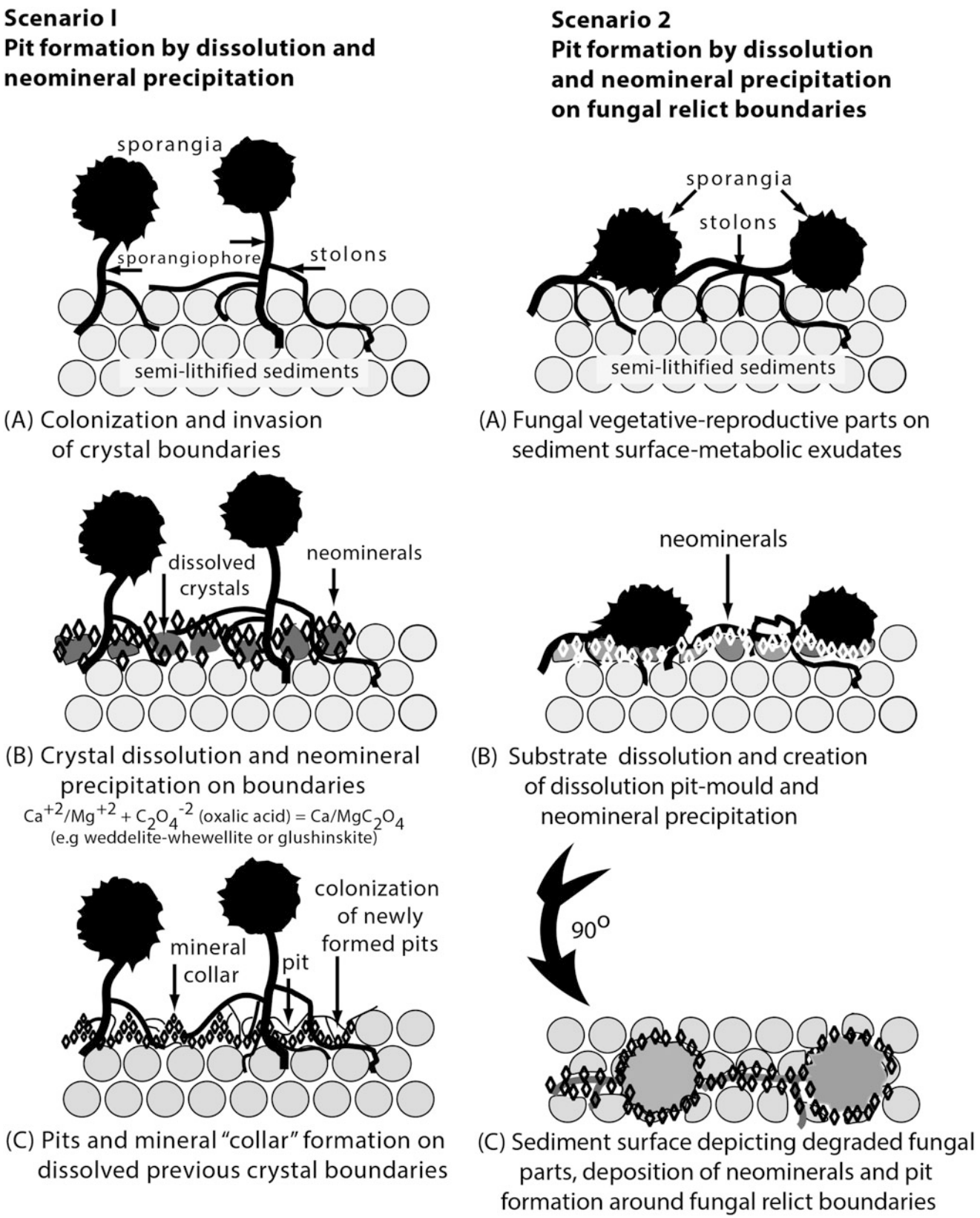

Fig. 5.11 Schematic figure showing a proposed two-pronged mechanism, for the three-stage pit formation, which could have worked separately or in combination. Scenario (1) involves fungal colonization of the Neoproterozoic substrate through hyphae-stolons and rhizoids invasion of the semi-lithified sediment surface penetrating it through grain boundaries resulting into grain dissolution, biominerals precipitating (mainly Ca/Mg-oxalates) and pits formation. The pits themselves become the target of new invasion by fungal hyphae. Scenario (2) envisages fungal vegetative parts (e.g sporangia, sporangiophores) spreading across the colonized substrate surface and with metabolic exudates released in the growth environment causing substrate dissolution, biomineral precipitation and molding the fungal parts within the substrate

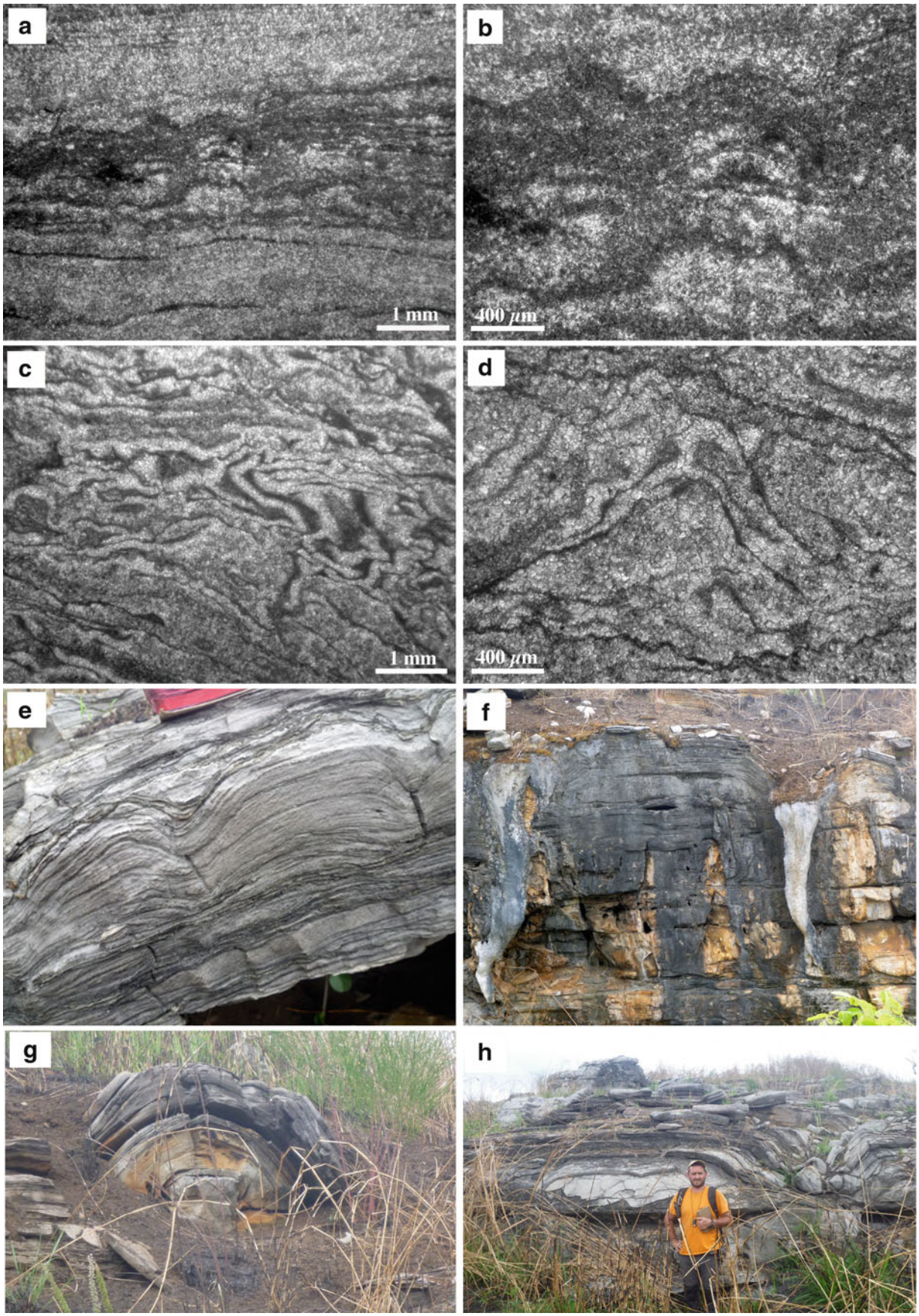

Fig. 5.12 (**a**, **b**) Images of flat laminated mats associated with stacked microstromatolitic laminae characterized by partially microsparitized thin organic-rich layers giving stratiform light layers. Thin section comes from a domal stromatolite (height 50 cm, wide 65 cm)

significant. The second scenario implies that fungal vegetative and reproductive parts (e.g., sporangia, sporangiophores) could spread across the colonized substrate surface and metabolic exudates that were released in the growth environment would have caused substrate dissolution, authigenic mineral precipitation and cementation of fungal parts within the substrate.

5.6 Implications

It is our contention that we have described here one of the earliest physical records of fungi, and that these organisms having inhabited the upper supratidal part of a shallowing-upward carbonate sequence. We also show how the fungi impacted the main petrophysical characteristics of the rock. Despite this importance and stratigraphic distribution, fungi are rarely reported in ancient series in the literature. This is particularly the case in the Precambrian of West Africa, where numerous stromatolites have been described in great details (Amard and Bertrand-Sarfati 1997). Clusters of closely packed meter-scale ellipsoid to upward expanding cone-shaped bioherms several meters (up to 5 m wide and 3 m thick, Fig. 5.12e–h) developed relief of several meters above the top of laminar microbial bindstone and small-sized LLH stromatolites associated with collapse breccia containing anhydrite relicts (Fig. 5.12). The biohermal level is 15 m-thick and belongs to the post-Marinoan Neoproterozoic SCIc unit (Schisto-Calcaire Group) recognized in the Niari Basin (the Republic of Congo) by Alvarez and Maurin (1991). The Niari Basin extends over more than 75,000 km^2 and is mainly constituted by two depressions, the Niari depression in the Republic of Congo and Nyanga depression in Gabon where the Mouila quarry is located. Study of the microbial contents (cyanobacteria and fungi) of the SCIc stromatolites is in progress (Yannick Callec and Alain Préat) and is focused on the lamina microstructure forming irregular bands and lenses of grey and light carbonate mud. They are associated with early diagenesis related to replacement by evaporitive brines (Fig. 5.12a–d).

The Mouila sediments were probably partly or totally lithified during early diagenesis through pervasive dolomitization in hypersaline brines allowing pits to be formed. In this very shallow environment (backslope of the levees and beach-ridge washovers) exposure was probably high, with very dry conditions proving favourable to fungal colonization. Numerous mudcracks seen in thin sections or under the SEM support this interpretation. Cyanobacteria are partly or entirely destroyed by the dolomicropar. This contrasts with the fungal hyphae which are reasonably well-preserved and intimately associated with the dolomicrospar and the dolomitized EPS that constituted an integral component of the original microbial mats.

Evidence for ancient life typically exists within sedimentary environments, where microbial mats and colonies of filamentous, coccoid or rod-shaped microbes have been found in Early Archean strata such as in cherts of the Pilbara and Barberton greenstone belts (Westall 2005). As fungi are increasingly pushed deeper into the Precambrian, their role in early Earth processes is also increasingly linked to two major events: the "Snowball Earth" and the rise of oxygenation in the Neoproterozoic (Heckman et al. 2001; Canfield 2005; Kennedy et al. 2006). How fungi may have impacted terrestrial weathering, and to what effect this may have played a role in the broader evolution of the Earth system remains unclear. We feel that this work takes a step further into the deep past by describing how fungal relicts within the Neoproterozoic Mouila series points towards their colonization and diagenesis of shallow sediments at the time.

Acknowledgements Kamal Kolo would like to thank Prof. Philippe Claeys, Department of Geology/Vrije Universiteit Brussels for supporting the experimental work in this study. We also thank the Department of Metallurgy/Vrije Universiteit Brussels for kindly giving access to their SEM and FE-SEM laboratories. The fieldwork was done under the terms of the SYSMIN program (Eighth Fonds Européen de Développement, BRGM-CGS-SANDER-MRAC). KOK would like to thank the Natural Sciences and Engineering Research Council of Canada for continued support. The authors thank Dr Yannick Callec, BRGM (Bureau Recherches Géologiques et Minières, Orléans, France) for guiding Alain Préat on the field in the Niari area during dry season (September 2012). We thank Prof. David Gillan for a comprehensive review which helped improve the MS.

Fig. 5.12 (continued) interstratified in strongly deformed, slumped evaporitic laminated dolomudstones (pictures **c** and **d**). Sample CB9, outcrop MAD8122-Yannick Callec, Republic of Congo, photo cb9252 and 9253/ap/2013). (**c**, **d**). Salt migration (slump, microenterolithe, folding -c, tepee -d) in a dolo-microsparitized mudstone with remnants of organic-rich microbial laminae. Same ouctrop as previous pictures, sample CB10 (50 cm above CB9), photo cb9258 and 9269/ap/2013). (**e**) Flat to slightly domal stromatolites switched between irregularly-laminated microbial dolomudstones. Outcrop MAD0165-Yannick Callec, Republic of Congo, photo P1170717/ap/2012). (**f**) Massive stromatolitic 'table' reef (height 2 m) bordered by recent tufa deposits, (**g**) Concentric sheet stromatolitic bioherm, (**h**) Stacked patch reef units flanked by intraclastic (angular stromatolitic chips) dolopackstones on both sides.(f–g–h) : same ouctcrop as (**e**), respectively photos P1170726/P1170734/ P1170744ap/2012). The stromatolites constitute a 15 m-thick level interstratified in well-bedded dolomudstones and ooid-pisoid dolopackstones and dolograinstones

References

Alexopoulos CJ, Mims CW (1979) Introductory mycology, 3rd edn. Wiley, New York

Alvarez P, Maurin JC (1991) Evolution sédimentaire et tectonique du bassin protérozoïque supérieur de Comba (Congo): stratigraphie séquentielle du Supergroupe Ouest-Congolien et modèle d'amortissement sur décrochements dans le contexte de la tectonogenèse panafricaine. Precambrian Res 50:137–171

Amard B, Bertrand-Sarfati J (1997) Microfossils in 2000 Ma old cherty stromatolites of the Franceville Group, Gabon. Precambrian Res 81:197–221

Bennett PC, Melcer ME, Siegel DI, Hassett JP (1988) The dissolution of quartz in dilute aqueous solutions of organic acids at 25°C. Geochim Cosmochim Acta 52:1521–1530

Berbee ML, Taylor JW (2001) Fungal molecular evolution: gene trees and geological time. In: McLaughin DJ, McLaughin EG, Lemke PA (eds) The Mycota VIIB systematic and evolution. Springer, Berlin, pp 229–245

Burford EP, Fomina M, Gadd GM (2003a) Fungal involvement in bioweathering and biotransformation of rocks and minerals. Miner Magaz 67:1127–1155

Burford EP, Kierans M, Gadd GM (2003b) Geomycology: fungi in mineral substrata. Mycologist 17:98–107

Butterfield NJ (2005) Probable proterozoic fungi. Paleobiology 31 (1):165–182

Canfield D (2005) The early history of atmospheric oxygen: Hommage to Robert A Garrels. Annu Rev Earth Planet Sci 33:1–36

Cardon Z, Whitbeck JL (eds) (2007) The rhizosphere. an ecological perspective. Elsevier Academic Press, New York, 212 pp

Cavagna S, Clari P, Martire L (1999) The role of bacteria in the formation of cold seep carbonates: geological evidence from Monferrato (Tertiary, NW Italy). Sediment Geol 126:253–270

Cavalier-Smith T (1987) The origin of fungi and pseudofungi. In: Rayner AM, Brasier CM, Moor D (eds) Evolutionary biology of the fungi. Cambridge University Press, Cambridge, pp 339–353

Cavalier-Smith T (2006) Cell evolution and Earth history: stasis and revolution. Philos Trans R Soc B: Biol Sci 361(1470):969–1006

Chen J, Blume HP, Beyer L (2000) Weathering of rocks induced by lichen colonization, a review. Catena 39(2):121–146

Clark DN (1980) The diagenesis of Zechstein carbonate sediments. In: Füchtbauer H, Peryt T (eds) The Zechstein Basin with emphasis on carbonate sequences. Stuttgart, E, Schweizerbart'sche Verlagsbuchandlung, Contribution to sedimentology, vol 9, pp 167–203

Esteban M, Klappa CF (1983) Subaerial exposure environment. In: Scholle P, Bebout DG, Moore CH (eds) Carbonate depositional environments, vol 33, American Association Petroleum Geolologists Memoir., pp 2–54

Feldmann M, McKenzie JA (1997) Messinian stromatolite-thrombolite associations, Santa Pola, SE Spain: an analogue for the Palaeozoic? Sedimentology 44:893–914

Gadd GM (1999) Fungal production of citric and oxalic acid: importance in metal speciation, physiology and biogeochemical processes. Adv Microb Physiol 41:47–92

Gadd GM (2007) Geomycology: biogeochemical transformations of rocks, minerals, metals and radionuclides by fungi, bioweathering and bioremediation. Mycol Res 111(1):3–49

Gérard G (1958) Carte géologique de l'Afrique Equatoriale Française au 2 000 000 avec notice explicative. Brazza. Direction Mines et Géologie. Afrique Equatoriale Française, 198 pp, 4 feuilles

Gerdes G, Krumbein W, Noffke N (2000) Evaporite microbial sediments. In: Riding R, Awramik S (eds) Microbial sediments. Springer, Berlin, pp 196–208

Golubic S, Gudrun R, Le Campion-Alsumard T (2005) Endolithic fungi in marine ecosystems. Trends Microbiol 13(5):229–235

Grote G, Krumbein WE (1992) Microbial precipitation of manganese by bacteria and fungi from desert rock and rock varnish. Geomicrobiol J 10:49–57

Grotzinger JP, Knoll AH (1999) Stromatolites in Precambrian carbonates: evolutionary mileposts and environmental dipsticks? Ann Rev Earth Planet Sci 27:313–358

Hardie LA (ed) (1977) Sedimentation on the modern carbonate tidal flats of Northwest Andros Island, Bahamas, vol 22. John Hopkins University Studies in Geology, Baltimore, 202 pp

Hardie LA, Ginsburg RN (1977) Layering: the origin and environmental significance of lamination and thin bedding. In: Hardie LA (ed) Sedimentation on the modern carbonate tidal flats of Northwest Andros Island, Bahamas, vol 22. John Hopkins University Studies in Geology, Baltimore, pp 50–12

Heckman DS, Geiser DM, Brooke RE, Rebecca L, Stauffer NL, Kardos S, Blair H (2001) Molecular evidence for the early colonization of land by fungi and plants. Science 293(5532):1129–1133

Hermann T, Podkovyrov V (2006) Fungal remains from the Late Riphean. Paleontolog J 40:207–214

Hoffland ET, Kuyper W, Wallander H, Plassard C, Gorbushina AA, Haselwandter K, Holmström S, Landeweert R, Lundström US, Rosling A, Sen R, Smits MM, van Hees PAW, van Breemen N (2004) The role of fungi in weathering. Front Ecol Environ 2(5):258–264

Jones B (2005) Dolomite crystal architecture: genetic implications for the origin of the tertiary Dolostones of the Cayman Islands. J Sediment Res 75:177–189

Kahle CF (1977) Origin of subaerial Holocene calcareous crusts: role of algae, fungi and sparmicritization. Sedimentology 24:413–435

Kendrick B (2000) The fifth kingdom, 3rd edn. Focus Publishing, R. Pullins Company, Newburyport, MA

Kennedy M, Droser M, Mayer LM, Pevear D, Mrofka D (2006) Late precambrian oxygenation; inception of the clay mineral factory. Science 311(5766):1446–1449

Kolo K, Claeys P (2005) In vitro formation of Ca-oxalates and the mineral glushinskite by fungal interaction with carbonate substrates and seawater. Biogeosciences 2:277–293

Kolo K, Keppens E, Préat A, Claeys P (2007) Experimental observations on fungal diagenesis of carbonate substrates. J Geophys Res Biogeosci 112, GO1007

Konhauser K (2007) Introduction to geomicrobiology. Blackwell Publishing, Malden, MA, 425 pp

Krings M, Taylor TN, Dotzler N (2013) Fossil evidence of the zygomycetous fungi. Persoonia 30:1–10

Krumbein WE (1972) Rôle des microorganismes dans la genèse, la diagenèse et la dégradation des roches en place. Revue Ecol Biol Sol 9:283–319

Krumbein WE, Jens K (1981) Biogenic rock varnishes of the Negev Desert (Israel): an ecological study of iron and manganese transformation by cyanobacteria and fungi. Oecologia 50:25–38

Logan BW, Rezak R, Ginsburg RN (1964) Classification and environmental significance of algal stromatolites. J Geol 72:68–83

Mamet B, Préat A (2005) Sédimentologie de la série viséenne d'Avesnes-sur-Helpe (Avesnois, Nord de la France). Geol Belgica 8:91–107

Moore-Landecker E (1991) Fundamentals of the fungi, 3rd edn. Prentice Hall, Englewood Cliffs, New Jersey, USA

Préat A, Kolo K, Mamet B, Gorbushina AA, Gillan DC (2003) Fossil and subrecent fungal communities in three calcrete series from the Devonian of the Canadian Rocky Mountains, Carboniferous of Northern France and Cretaceous of Central Italy. In: Krumbein WE, Paterson DM, Zavarzin GA (eds) Fossil and recent biofilm. A natural history of life on Earth. Kluwer Acad. Publ., pp 291–306

Préat A, Kolo K, Delpomdor F (2010) A peritidal evaporate environment in the Neoproterozoic of South Gabon (Schisto-Calcaire Subgroup). Precambrian Res 177:253–265

Préat A, Prian JP, Thiéblemont D, Obame RM, Delpomdor F (2011a) Stable isotopes of oxygen and carbon compositions in the Neoproterozoic of South Gabon (Schisto-Calcaire Subgroup, Nyanga Basin): are cap carbonates and lithoherms recording a particular destabilization event after the Marinoan glaciation? J Afr Earth Sci 60:273–287

Préat A, Delpomdor F, Kolo K, Gillan D, Prian JP (2011b) Stromatolites and cyanobacterial mats in peritidal evaporitive environments in the Neoproterozoic of Bas-Congo (Democratic Republic of Congo) and South Gabon. In: Seckbach J, Tewari VC (eds) Stromatolites: interaction of microbes with sediments, Series: cellular origin, life in extreme habitats and astrobiology. Springer, Heidelberg, pp 43–63. doi:10.1007/978-94-007-0397

Purser BH (ed) (1973) The Persian Gulf. Holocene carbonate sedimentation and diagenesis in a shallow epicontinental Sea. Springer, Berlin, Heidelberg, New York, 471 pp

Redecker D, Kodner R, Graham LE (2000) Glomalean fungi from the Ordovician. Science 289(5486):1920–1921

Richter DD, Oh NH, Fimmen R, Jason J (2007) The rhizosphere and soil formation. In: Cardon Z, Whitbeck JL (eds) The rhizosphere. An ecological perspective. Elsevier Academic Press, pp 179–200

Saylor BZ, Kaufman AJ, Grotzinger JP, Urban F (1998) A composite reference section for terminal Proterozoic strata of Southern Namibia. J Sedim Res 68(6):1223–1235

Sellwood BW (1986) Shallow-marine carbonate environments. In: Reading HG (ed) Sedimentary environments and facies. Blackwell Science Publ, Oxford, pp 283–234

Sterflinger K (2000) Fungi as geologic agents. Geomicrobiol J 17:97–124

Sterfinger K, Krumbein WE (1997) Dematiaceous fungi as a major agent for biopitting on Mediterranean marbles and limestones. Geomicrobiol J 14:219–230

Stubblefield SP, Taylor TN (1988) Recent advances in palaeomycology. New Phytol 108:3–25

Taylor TN, Hass H, Kerp H, Krings M, Hanlin RT (2005) Perithecial ascomycetes from the 400 million year old Rhynie chert: an example of ancestral polymorphism. Mycologia 97:269–285

Thiéblemont D, Castaing C, Billa M, Bouton P, Préat A (2009) Notice explicative de la Carte géologique et des Ressources minérales de la République gabonaise à 1/1 000 000, Editions DGM, Ministère des Mines et du Pétrole, des Hydrocarbures, Libreville, 381 pp

Vahrenkamp VC, Swart PK (1994) Late Cenozoic sea-water generated dolomites of the Bahamas: metastable analogues for the genesis of ancient platform dolomites, In: Purser BH, Tucker ME, Zenger DH (eds) Dolomites, a volume in honour of Dolomie, vol 21, Special Publication. International Association of Sedimentologists, pp 133–153

Verrecchia EP (2000) Fungi and Sediments. In: Riding R, Awramik S (eds) Microbial sediments. Springer, Berlin, pp 68–75

Verrecchia EP, Loisy C, Braissant O, Gorbushina AA (2003) The role of fungal biofilm and networks in the terrestrial calcium carbonate cycle. In: Krumbein WE, Paterson DM, Zavarzin GA (eds) Fossil and recent biofilm. A natural history of life on Earth. Kluwer Ac. Publ., pp 363–369

Veizer J, Plumb KA, Clayton RN, Hinton RW, Grotzinger JP (1992) Geochemistry of Precambrian carbonates: V. Late Paleoproterozoic seawater. Geochim Cosmochim Acta 56:2487–2501

Vogel K, Gektidis M, Golubic S, Kiene WE, Radtke G (2000) Experimental studies on microbial bioerosion at Lee Stocking Island, Bahamas and One Tree Island, Great Barrier Reef, Australia: implications for paleoecological reconstructions. Lethaia 33:190–204

Walter MR (ed) (1976) Stromatolites. Developments in sedimentology, vol 20. Elsevier, Amsterdam, Oxford, New York, 790 pp

Welch SA, Barker WW, Banfield JF (1999) Microbial extracellular polymers and plagioclase dissolution. Geochim Cosmochim Acta 57:2939–2948

Westall F (2005) Early life on Earth: the ancient fossil record, astrobiology: future perspectives. pp 287–316

Wright VP (1986) The role of fungal biomineralization in the formation of Early Carboniferous soil fabrics. Sedimentology 33:831–838

Yuan X, Xiao S, Taylor TN (2006) Lichen-like symbiosis 600 million years ago. Science 308(5724):1017–1020